Clinical Infectious Diseases

MAJOR ARTICLE

Surgical Mask Partition Reduces the Risk of Noncontact Transmission in a Golden Syrian Hamster Model for Coronavirus Disease 2019 (COVID-19)

Jasper Fuk-Woo Chan,[1,2,3,a] Shuofeng Yuan,[1,a] Anna Jinxia Zhang,[1,a] Vincent Kwok-Man Poon,[1] Chris Chung-Sing Chan,[1] Andrew Chak-Yiu Lee,[1] Zhimeng Fan,[1] Can Li,[1] Ronghui Liang,[1] Jianli Cao,[1] Kaiming Tang,[1] Cuiting Luo,[1] Vincent Chi-Chung Cheng,[3] Jian-Piao Cai,[1] Hin Chu,[1] Kwok-Hung Chan,[1] Kelvin Kai-Wang To,[1,2,3] Siddharth Sridhar,[1,2,3] and Kwok-Yung Yuen[1,2,3]

[1]State Key Laboratory of Emerging Infectious Diseases, Carol Yu Centre for Infection, Department of Microbiology, Li Ka Shing Faculty of Medicine, The University of Hong Kong, Pokfulam, Hong Kong Special Administrative Region, China, [2]Department of Clinical Microbiology and Infection Control, The University of Hong Kong-Shenzhen Hospital, Shenzhen, Guangdong, China, and [3]Department of Microbiology, Queen Mary Hospital, Pokfulam, Hong Kong Special Administrative Region, China

Background. Coronavirus disease 2019 (COVID-19) caused by severe acute respiratory syndrome coronavirus 2 (SARS-CoV-2) is believed to be mostly transmitted by medium- to large-sized respiratory droplets, although airborne transmission may be possible in healthcare settings involving aerosol-generating procedures. Exposure to respiratory droplets can theoretically be reduced by surgical mask usage. However, there is a lack of experimental evidence supporting surgical mask usage for prevention of COVID-19.

Methods. We used a well-established golden Syrian hamster SARS-CoV-2 model. We placed SARS-CoV-2-challenged index hamsters and naive hamsters into closed system units each comprising 2 different cages separated by a polyvinyl chloride air porous partition with unidirectional airflow within the isolator. The effect of a surgical mask partition placed between the cages was investigated. Besides clinical scoring, hamster specimens were tested for viral load, histopathology, and viral nucleocapsid antigen expression.

Results. Noncontact transmission was found in 66.7% (10/15) of exposed naive hamsters. Surgical mask partition for challenged index or naive hamsters significantly reduced transmission to 25% (6/24, $P = .018$). Surgical mask partition for challenged index hamsters significantly reduced transmission to only 16.7% (2/12, $P = .019$) of exposed naive hamsters. Unlike the severe manifestations of challenged hamsters, infected naive hamsters had lower clinical scores, milder histopathological changes, and lower viral nucleocapsid antigen expression in respiratory tract tissues.

Conclusions. SARS-CoV-2 could be transmitted by respiratory droplets or airborne droplet nuclei which could be reduced by surgical mask partition in the hamster model. This is the first in vivo experimental evidence to support the possible benefit of surgical mask in prevention of COVID-19 transmission, especially when masks were worn by infected individuals.

Keywords. coronavirus; COVID-19; SARS-CoV-2; mask; transmission.

The source of the 2003 severe acute respiratory syndrome (SARS) epidemic was traced to civets in live animal markets and ultimately to Chinese horseshoe bats in the wild [1–3]. The epidemiological significance of the large number of bat SARS-related coronaviruses subsequently found in horseshoe and other bat species was not fully appreciated for the last 17 years [4, 5]. In late 2019, infection due to a novel *betacoronavirus* named severe acute respiratory syndrome coronavirus 2 (SARS-CoV-2), which is phylogenetically close to bat SARS-related coronaviruses, was reported in patients with epidemiological link to a market with wild mammal trade in Wuhan, China [6–8]. SARS-CoV-2 infection causing coronavirus disease 2019 (COVID-19) was initially recognized as an acute febrile pneumonia with lymphopenia and multifocal peripheral ground glass changes on thoracic computerized tomography [9–11]. COVID-19 is often self-limiting but may have severe manifestations such as silent (asymptomatic until sudden collapse) hypoxia, acute respiratory distress syndrome (ARDS), thrombocytopenia, and disseminated intravascular coagulation with diffuse microvascular thrombosis, deep venous thrombosis with pulmonary embolism, and/or multi-organ failure [9, 10, 12, 13]. Gastrointestinal manifestations such as diarrhea, neurological manifestations such as meningoencephalitis and Guillain-Barré syndrome, and Kawasaki syndrome-like multisystemic inflammatory disorder in children have also been reported [14–16]. However, most symptomatic patients have mild to moderate respiratory illness with manifestations such as rhinorrhea, sore throat, cough, conjunctivitis, anosmia, and ageusia [17, 18]. Furthermore, a high proportion of patients with COVID-19 have subclinical or mildly symptomatic infections, which is believed to enable efficient person-to-person

Received 12 May 2020; editorial decision 14 May 2020; accepted 28 May 2020; published online May 30, 2020.

[a]J. F-W. C., S. Y., and A. J. Z. contributed equally to this work.

Correspondence: K.-Y. Yuen, State Key Laboratory of Emerging Infectious Diseases, Carol Yu Centre for Infection, Department of Microbiology, Li Ka Shing Faculty of Medicine, The University of Hong Kong, Pokfulam, Hong Kong Special Administrative Region, China (kyyuen@hku.hk).

Clinical Infectious Diseases® 2020;71(16):2139–49

DOI: 10.1093/cid/ciaa644

transmission in both community and hospital settings. This renders symptom screening at borders ineffective, entails extensive testing and isolation of infected individuals, requires labor-intensive contact tracing measures, and necessitates social distancing or lockdowns. As a result, the ongoing COVID-19 pandemic has already affected more than 4 million patients with over 280 000 deaths in just 5 months [19].

Although COVID-19 is believed to be transmitted by respiratory droplet and direct or indirect contact, no clear experimental evidence for this has been reported. Based on in silico estimates of the binding affinity of angiotensin-converting enzyme 2 (ACE2) of common laboratory mammals and the receptor-binding domain of the surface spike protein of SARS-CoV-2, we recently established a golden Syrian hamster model for COVID-19 [20]. SARS-CoV-2-infected hamsters developed clinical signs of rapid breathing, weight loss, and histopathological changes of ARDS [20]. Using this animal model, we showed that SARS-CoV-2-challenged index hamsters consistently infected cohoused naive hamsters, confirming virus transmission by direct or indirect contact [20]. However, the controversies of whether there is transmission by respiratory droplets or airborne droplet nuclei, and whether the wearing of surgical mask by the virus shedder or by the susceptible individual is useful for the prevention of transmission, are still unsettled. In this study, using our hamster model for COVID-19, we confirmed noncontact transmission of SARS-CoV-2, which could potentially be prevented by surgical mask partition between the infected and the exposed susceptible host.

METHODS

Virus and Biosafety

SARS-CoV-2 was isolated from the nasopharyngeal aspirate specimen of a laboratory-confirmed COVID-19 patient in Hong Kong [21]. The plaque purified viral isolate was amplified by 1 additional passage in VeroE6 cells to make working stocks of the virus as described previously [21]. All experiments involving live SARS-CoV-2 followed the approved standard operating procedures of the Biosafety Level (BSL)-3 facility of The University of Hong Kong (HKU) [22, 23].

Animals

Approval was obtained from the HKU Committee on the Use of Live Animals in Teaching and Research. Male and female Syrian hamsters, aged 6–10 weeks old, were obtained from the Chinese University of Hong Kong Laboratory Animal Service Centre through the HKU Laboratory Animal Unit. The animals were kept in BSL-2 housing and given access to standard pellet feed and water ad libitum until virus challenge in our BSL-3 animal facility. The animal rooms were kept at 25°C and 50% humidity.

Noncontact Transmission Model Set-Up

To study the transmissibility of SARS-CoV-2 among hamsters through noncontact transmission, we housed SARS-CoV-2-challenged index hamsters and naive hamsters together in closed systems. The closed systems were kept in isolators (Tecniplast SpA, Varese, Italy) to prevent leakage of contaminated air to

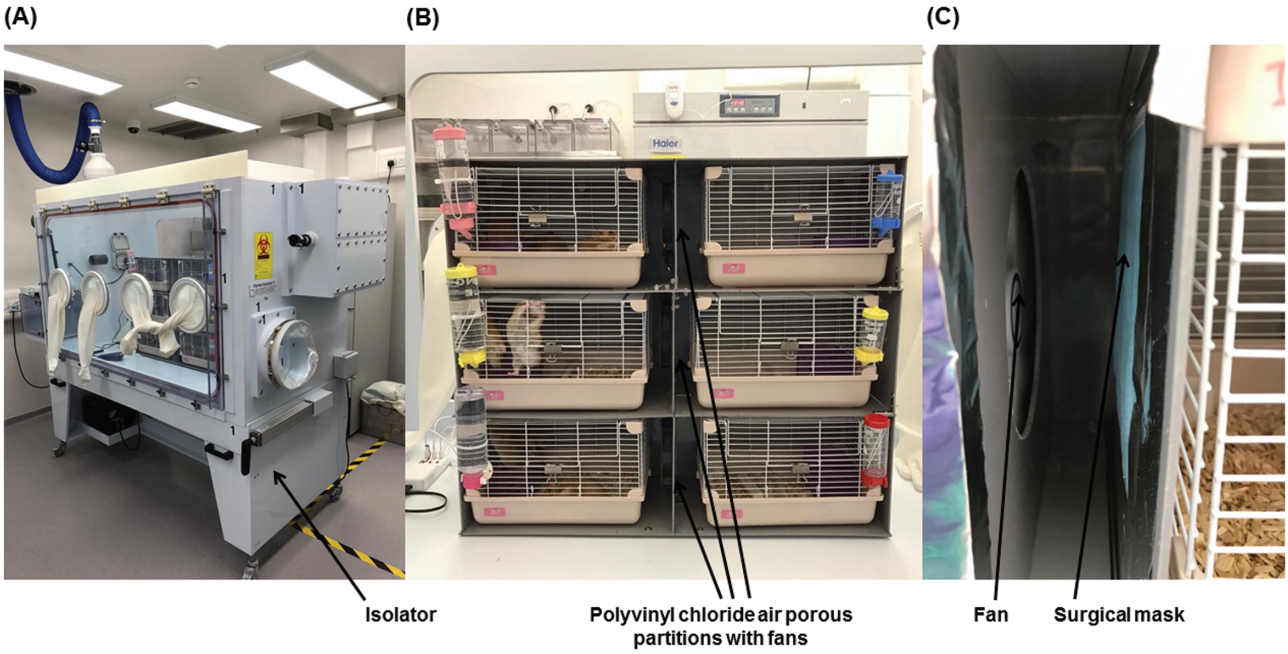

Figure 1. Noncontact transmission of SARS-CoV-2 in the Syrian hamster model. *A*, The closed systems housing the hamsters were placed in the isolator in a Biosafety Level-3 laboratory. *B*, Enlarged view of the closed systems used in the noncontact transmission studies. Each system contained 2 cages (left and right) separated by a polyvinyl chloride air porous partition. An electrically powered fan was installed at the polyvinyl chloride air porous partition to ensure unidirectional airflow from the cage housing the challenged index hamster to the cage housing the naive hamsters. *C*, Surgical mask partition with the blue external surface facing the challenged hamsters in experiment 3. Abbreviation: SARS-CoV-2, severe acute respiratory syndrome coronavirus 2.

the external environment (Figure 1A). Each closed system contained 2 cages (Marukan Co., Ltd., Osaka, Japan) separated by a polyvinyl chloride air porous partition with unidirectional airflow maintained by an electrically powered fan from the cage housing 1 SARS-CoV-2-challenged index hamster toward the cage housing 3 naive hamsters (Figure 1B). Each system had either no surgical mask partition or a layer of partition made of surgical mask (A. R. Medicom Inc. [Asia] Ltd., Hong Kong, China) fulfilling the ASTM F2100 Level 1 standard tightly sealed onto the polyvinyl chloride air porous partition between the cages to assess the effect of the surgical mask partition in this hamster model (Figure 1C). There were 2 or 3 closed systems per isolator.

Animal Challenge and Transmission Experiments

Three sets of experiments were conducted using our isolator noncontact transmission model. In the first experiment, no mask partition was placed between the two cages in each system to investigate whether noncontact transmission occurred among the hamsters (Figure 2). A total of 5 systems housing 20 hamsters were included in the first experiment. In the second experiment, to simulate the situation when a surgical mask is worn by a SARS-CoV-2-infected person, a partition layer using surgical mask was placed on the polyvinyl chloride air porous partition between the cages with the outer fluid-repellent layer (the blue side) facing the exposed naive hamsters to prevent emission of exhaled respiratory droplets containing SARS-CoV-2 from the challenged index hamster to infect the exposed naive hamsters (Figure 3A). A total of 4 systems housing 16 hamsters were included in the second experiment. In the third experiment, to simulate the situation when close contacts of a SARS-CoV-2-infected person wear surgical masks, the surgical mask partition with the outer fluid-repellent layer facing the challenged index hamsters was placed on the polyvinyl chloride air porous partition between the cages to prevent droplets containing SARS-CoV-2 exhaled by the challenged index hamster from being inhaled by the exposed naive hamsters (Figure 3B). A total of 4 systems housing 16 hamsters were included in the third experiment. The air velocities from the challenged index hamster's cage to the exposed naive hamsters' cage in the 3 experiments were shown in Table 1.

At day 0, a challenge dose of 100 µL of Dulbecco's Modified Eagle Medium (DMEM) containing 10^5 plaque-forming units of SARS-CoV-2 was intranasally inoculated to the index hamster in each system under intraperitoneal ketamine (200 mg/kg) and xylazine (10 mg/kg) anesthesia as we described previously [20]. Twenty-four hours later, 3 naive hamsters were transferred to the cage adjacent and exposed to the cage housing the virus-challenged index hamster in each system. The animals were monitored daily for clinical signs of disease. Two of the 3 exposed naive hamsters in each system were sacrificed at 5 days postinoculation (dpi) (4 days after exposure). The challenged index hamster and remaining exposed naive

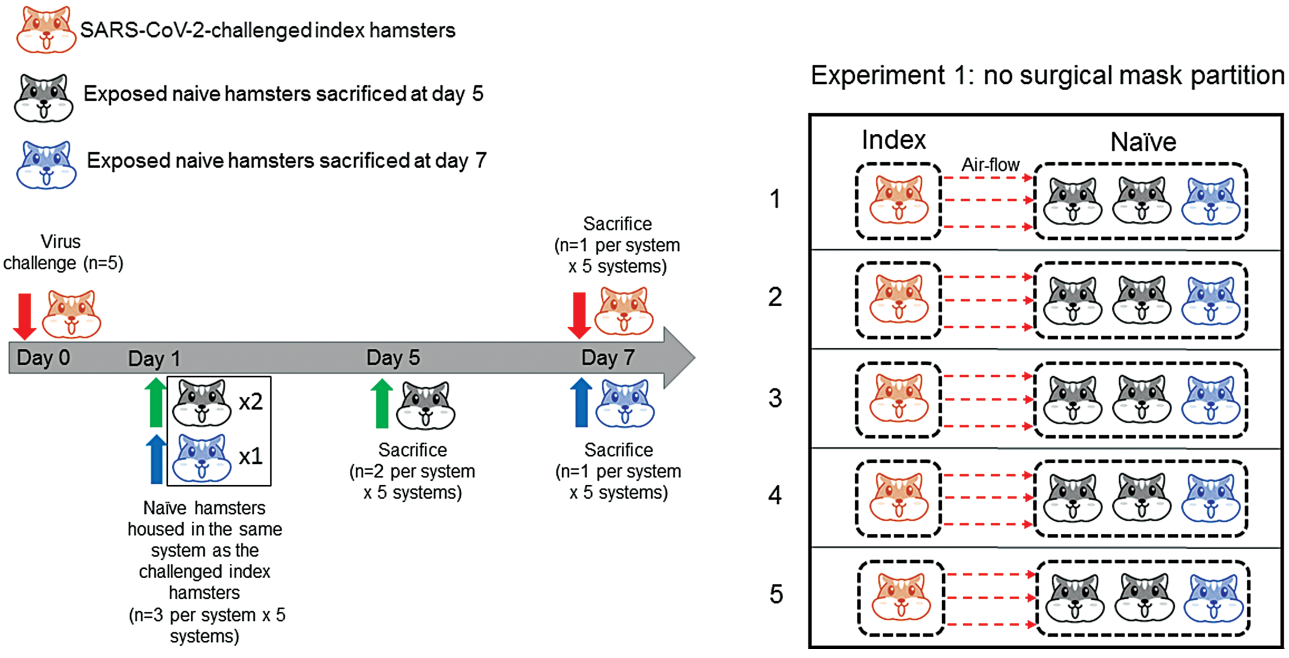

Figure 2. Noncontact transmission of SARS-CoV-2 from virus-challenged index hamsters to exposed naive hamsters without surgical mask partition between the cages (experiment 1). SARS-CoV-2 was intranasally inoculated to the index hamsters (n = 5) at day 0. Twenty-four hours later, 3 naive hamsters were transferred to the adjacent cage and exposed to the cage housing the virus-challenged index hamster. Two exposed naive hamsters in each system were sacrificed at 5 dpi (4 days after exposure). The challenged index hamster and the remaining exposed naive hamster in each system were then sacrificed at 7 dpi. A total of 5 systems (n = 20) were included in experiment 1. Abbreviation: dpi, days postinoculation; SARS-CoV-2, severe acute respiratory syndrome coronavirus 2.

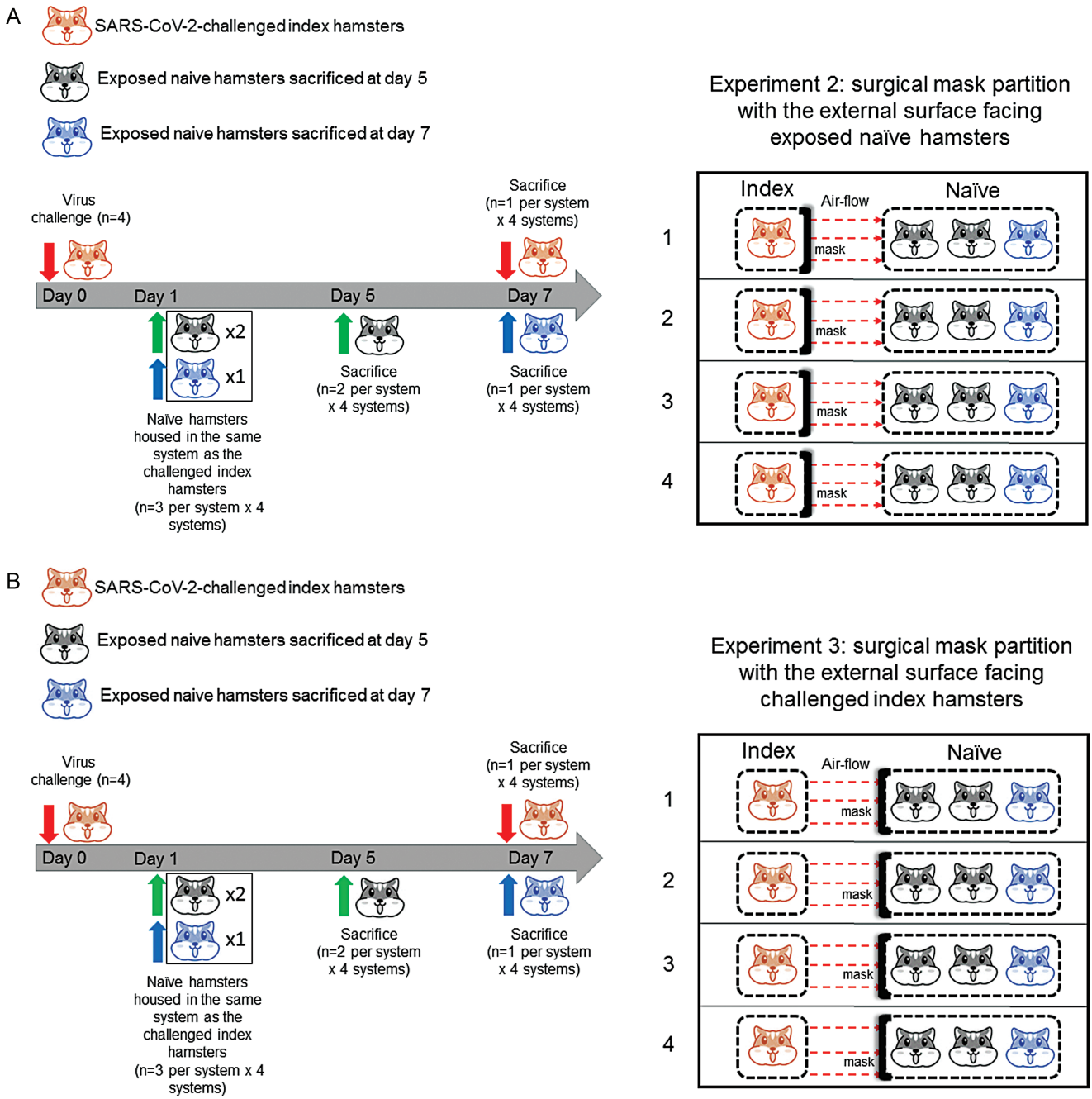

Figure 3. Noncontact transmission of SARS-CoV-2 from virus-challenged index hamsters to exposed naive hamsters with surgical mask partition between the cages. Surgical mask partition with the external surface facing *A*, exposed naive hamsters (experiment 2) to mimic the situation of the mask being worn by the challenged index hamster for preventing the emission of exhaled SARS-CoV-2-infected droplets or *B*, facing the challenged index hamsters to mimic the situation of the mask being worn by the naive hamsters to prevent the reception and inhalation of SARS-CoV-2-infected droplets from the challenged index hamsters. The timing of virus challenge and sacrifice of animals was the same as in experiment 1. A total of 4 systems (n = 16) were included in experiment 2, and another 4 systems (n = 16) were included in experiment 3. Abbreviation: SARS-CoV-2, severe acute respiratory syndrome coronavirus 2.

hamster in each system were then sacrificed at 7 dpi. The animals' organ tissues collected at necropsy were separated into 2 parts, one immediately fixed in 10% phosphate-buffered saline formalin for histopathological analysis, and the other immediately frozen at −80°C until use for viral load studies as we described previously [20, 24, 25]. Serum samples were used for neutralizing antibody detection as we described previously [20]. To compare the histopathological changes at 5 dpi, an additional control SARS-CoV-2-challenged hamster was sacrificed at 5 dpi.

Table 1. Air Velocity from the Challenged Index Hamsters' Cages to the Exposed Naive Hamsters' Cages With or Without Surgical Mask Partition

Group	Air Velocity From the Challenged Index Hamster's Cage to the Exposed Naive Hamsters' Cage (m/s)[a]
Experiment 1: No mask	0.676 ± 0.107
Experiment 2: Masked index	0.335 ± 0.070
Experiment 3: Masked naive	0.428 ± 0.028

[a]The values represent the mean air velocity ± standard deviations.

Statistical Analysis

All data were analyzed with GraphPad Prism software (GraphPad Software, Inc). Fisher exact test was used to compare the rate of infection between the different groups of hamsters with or without surgical mask partition. Student *t*-test was used to determine significant differences in clinical scores and virus loads between different groups [20]. $P < .05$ was considered statistically significant.

RESULTS

Noncontact Transmission of SARS-CoV-2 Among Hamsters

Consistent with our previous findings, all 13 (n = 5, 4, and 4 for experiments 1, 2, and 3, respectively) SARS-CoV-2-challenged index hamsters developed clinical signs of lethargy, ruffled furs, hunched back posture, and rapid breathing starting at 2 dpi, and had virological and histological evidence of infection [20]. In the first experiment, 6 of the 10 (60%) exposed naive hamsters sacrificed at 5 dpi (4 days after exposure) also developed similar clinical signs. The overall mean clinical score of the 10 exposed naive hamsters was 1.800 ± 1.687 (Table 2). The 6 naive hamsters that developed clinical signs were confirmed to be infected with SARS-CoV-2 as evidenced by positive reverse transcription polymerase chain reaction (RT-PCR) results (Table 3). The viral loads ranged from around 0.1 to 1000 genome copies/β-actin (nasal turbinate), 0.1 to 100 genome copies/β-actin (trachea), and 0.01 to 10 genome copies/β-actin (lung) (Figure 4A). At 7 dpi (6 days after exposure), the remaining 5 naive hamsters had a mean clinical score of 2.400 ± 1.517. Four of the 5 (80.0%) exposed naive hamsters were found to be infected, with viral loads of around 100 to 1000 genome copies/β-actin (nasal turbinate), 10 to 100 genome copies/β-actin (trachea), and 0.1 to 100 genome copies/β-actin (lung) (Figure 4B). At both 5 dpi and 7 dpi, the viral loads were generally highest in the nasal turbinate and lowest in the lung. None of the index and naive hamsters died.

Noncontact Transmission of SARS-CoV-2 Among Hamsters With Surgical Mask Partition

Having demonstrated that noncontact transmission of SARS-CoV-2 occurred among the hamsters in our model, we next investigated the effectiveness of surgical mask partition to reduce the risk of noncontact transmission. Surgical mask partition between cages was installed with the external fluid-repelling surface facing the exposed naive hamsters or the challenged index hamsters to mimic the situation of the mask being worn by index hamsters or by exposed naive contact hamsters, respectively.

In the second experiment in which the external surface of the mask was facing the naive hamsters, at 5 dpi (4 days after exposure), 2 of the 3 naive hamsters in each system (n = 8) were sacrificed. Only 1 out of 8 (12.5%) naive hamsters was SARS-CoV-2 RT-PCR-positive (Table 3). The viral loads of this hamster were about 1 (nasal turbinate), 100 (trachea), and 10 (lung) genome copies/β-actin (Figure 4A). At 7 dpi, the remaining exposed naive hamster (n = 4) and the SARS-CoV-2-challenged index hamster (n = 4) in each system were also sacrificed. Only 1 of the 4 (25.0%) remaining naive hamsters were RT-PCR-positive, with viral loads of around 0.5 (lung) to 100 (nasal turbinate) genome copies/β-actin (Figure 4B). This transmission rate (2/12, 16.7%) was significantly ($P = .019$) lower than that of the exposed naive hamsters without surgical mask partition (10/15, 66.7%).

In the third experiment, the external surface of the mask was facing the challenged index hamsters. At 5 dpi (4 days after exposure), 2 of the 3 naive hamsters in each system (n = 8) were sacrificed. Three out of 8 (37.5%) exposed naive hamsters developed clinical signs and were SARS-CoV-2 RT-PCR positive (Table 3). The viral loads ranged from around 1 to 10 genome copies/β-actin (nasal turbinate), 0.01 to 100 (trachea) genome copies/β-actin, and 0.001 to 10 genome copies/β-actin (lung) (Figure 4A). At 7 dpi, the remaining exposed naive hamster (n = 4) and the challenged index hamster (n = 4) in each system were also sacrificed. One of the 4 (25.0%) remaining naive hamsters were RT-PCR positive, with viral loads of around 1 (lung) to 100 (nasal turbinate) genome copies/β-actin (Figure 4B). This transmission rate (4/12, 33.3%) was also lower than that of the exposed naive hamsters without surgical

Table 2. Clinical Scores of Exposed Naive Hamsters With or Without Surgical Mask Partition

Group	5 dpi[a]	*P*-value[b]	7 dpi[a]	*P*-value[b]
Naive (no mask)	1.800 ± 1.687		2.400 ± 1.517	
Naive (any mask)	0.313 ± 0.793	.036	0.375 ± 0.744	.008
Naive (masked index)	0.000 ± 0.000	.008	0.250 ± 0.500	.031
Naive (masked naive)	0.625 ± 1.061	.107	0.500 ± 1.000	.069

Abbreviation: dpi, days postinoculation.

[a]A score of 1 was given to each of the following clinical signs: lethargy, ruffled fur, hunched back posture, and rapid breathing.

[b]*P*-values represent comparison between the naive (no mask) group with the other groups (Student *t*-test). The values represent the mean clinical scores ± standard deviations.

Table 3. Noncontact Transmission Rate From Challenged Hamsters to Exposed Naive Hamsters With or Without Surgical Mask Partition Detected by RT-PCR[a]

Group	5 dpi	*P*-value[a]	7 dpi	*P*-value[a]	Total	*P*-value[a]
Naive (no mask)	6/10 (60.0%)		4/5 (80.0%)		10/15 (66.7%)	
Naive (any mask)	4/16 (25.0%)	.109	2/8 (25.0%)	.103	6/24 (25.0%)	.018
Naive (masked index)	1/8 (12.5%)	.066	1/4 (25.0%)	.206	2/12 (16.7%)	.019
Naive (masked naive)	3/8 (37.5%)	.637	1/4 (25.0%)	.206	4/12 (33.3%)	.128

Abbreviation: dpi, days postinoculation.

[a]*P*-values represent comparison between the naive (no mask) group with the other groups (Fisher exact test).

mask partition (10/15, 66.7%), although not reaching statistical significance ($P = .128$).

Immunological Response in Hamsters Infected by SARS-CoV-2 Through Noncontact Transmission

At 7 dpi (6 days after exposure of the naive hamsters to the challenged index hamsters), all challenged index hamsters (n = 13) exhibited high titers of serum neutralizing antibodies, ranging from 1:320 to ≥1:640, which is consistent with our previous observation (Figure 5). Interestingly, 3 of the 5 exposed (60%) naive hamsters without surgical mask partition sacrificed at 7 dpi also developed serum neutralizing antibody titers of 1:160 to 1:640, which suggested that these 3 RT-PCR-positive infected naive hamsters likely acquired the virus very early after exposure to the challenged index hamsters as it required 5–7 days before serum neutralizing antibodies were detectable in this animal model. In contrast, none of the 8 exposed naive hamsters with surgical mask partition facing either side sacrificed at 7 dpi, including the 2 RT-PCR-positive hamsters, developed detectable serum neutralizing antibody (all <1:20). These results suggested that even though these 2 exposed naive hamsters were infected, they likely acquired the virus much later than the infected naive hamsters without protection by surgical mask partition.

Histological Features of Hamsters Infected by SARS-CoV-2 Through Noncontact Transmission

The representative histological and immunofluorescent staining findings of the infected naive hamsters are shown in Figure 6. At 5 dpi (4 days after exposure), the histopathological changes of the infected naive hamsters in experiments 1, 2, and 3 were generally milder than those of the challenged control hamster. In the infected naive hamsters, the nasal turbinate only showed mild degree of epithelial cell swelling and submucosal infiltration, whereas there were severe epithelial cell death, desquamation, and massive submucosal infiltration in the challenged control hamster (Figure 6A, a to d). Similarly,

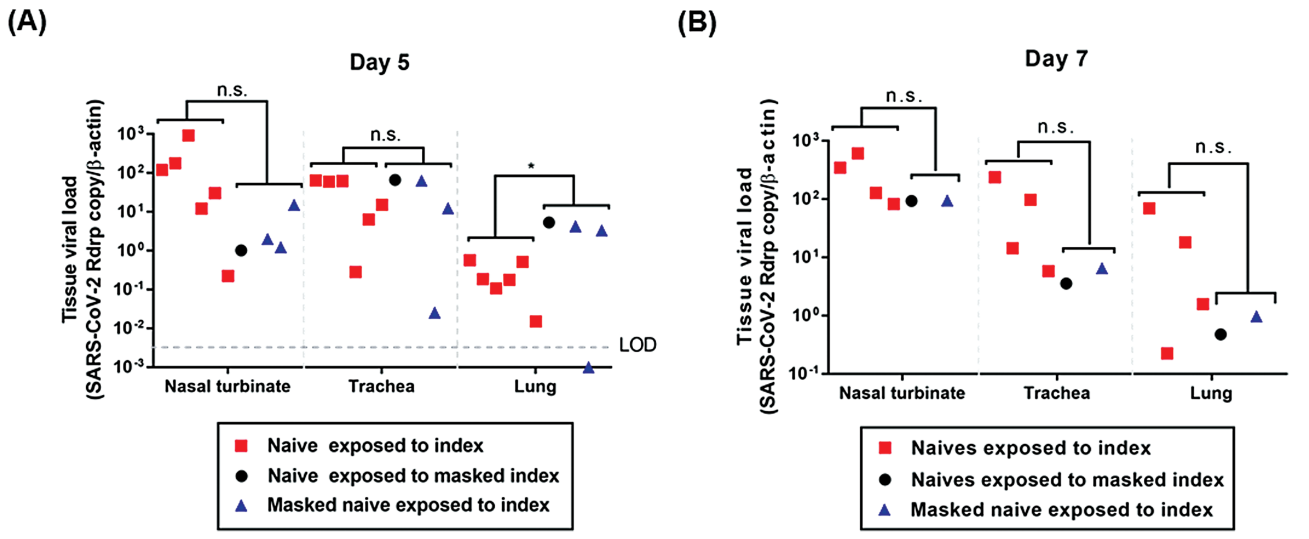

Figure 4. Viral loads in the respiratory tract tissues of the SARS-CoV-2 RT-PCR-positive naive hamsters exposed to the challenged index hamsters. Naive hamsters without surgical mask partition in experiment 1 (squares), naive hamsters exposed to masked challenged index hamsters in experiment 2 (circles), and the masked naive hamsters exposed to the challenged index hamsters in experiment 3 (triangles). *A*, Day 5 and *B*, day 7 post-challenge of index hamsters. Statistical comparison between the SARS-CoV-2 RT-PCR-positive naive hamsters without surgical mask partition (experiment 1) and the SARS-CoV-2 RT-PCR-positive naive hamsters with surgical mask partition (experiments 2 and 3) was performed using Student *t*-test. *$P < .05$. Abbreviations: LOD, limit of detection; ns, not significant; RT-PCR, reverse transcription-polymerase chain reaction; SARS-CoV-2, severe acute respiratory syndrome coronavirus 2.

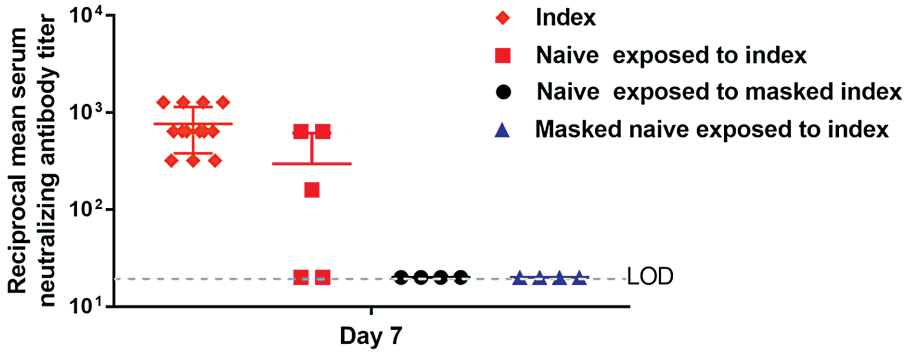

Figure 5. Reciprocal serum SARS-CoV-2-specific neutralizing antibody titers in the hamsters. The mean serum neutralizing antibody titers of the challenged index hamsters (n = 13, diamonds), the naive hamsters exposed to the challenged index hamsters without surgical mask partition in experiment 1 (n = 5, squares), the naive hamsters exposed to masked challenged index hamsters in experiment 2 (n = 4, circles), and the masked naive hamsters exposed to the challenged index hamsters in experiment 3 (n = 4, triangles) at day 7 post-challenge of the index hamsters (6 days after exposure of the naive hamsters to the index hamsters) are shown on a logarithmic scale. Dotted line indicates the lower limit of detection (<1:20). Abbreviation: LOD, limit of detection.

the histopathological changes in the trachea (Figure 6A, e to h) and lung (Figure 6A, i to l) of the challenged control hamster were generally more severe than the infected naive hamsters in experiments 1, 2, and 3. This was corroborated by the viral N antigen expression pattern (Figure 6B).

DISCUSSION

Following up on the demonstration of SARS-CoV-2 transmission through direct or indirect contact in our hamster model, a noncontact transmission model inside isolators was established in this study [20]. We showed that noncontact transmission occurred in 66.7% of unprotected naive hamsters after exposure to SARS-CoV-2-challenged hamsters for ≤96 hours. Despite documented transmission in the exposed naive hamsters as evident by positive viral loads in the upper and lower respiratory tract at 4 days after exposure or serum neutralizing antibody titer at 6 days after exposure, these hamsters had less severe histopathological changes and lower amount of SARS-CoV-2-N antigen expression in the upper and lower respiratory tract compared to virus-challenged hamsters. Moreover, the use of surgical mask partition to prevent emission of exhaled respiratory droplets from SARS-CoV-2-challenged index hamsters significantly reduced the transmission rate to 16.7% ($P = .019$). The use of surgical mask partition to protect naive hamsters reduced the transmission rate to 33.3%, although this did not reach statistical significance, likely because of the relatively small number of animals ($P = .128$). As expected, the histopathological changes and the amount of respiratory tract viral N antigen expression of these protected naive hamsters were also significantly lower than those of the challenged index hamsters.

The finding of SARS-CoV-2 being transmitted by the noncontact route of respiratory droplets or airborne droplet nuclei is not unexpected as this is also the case for other respiratory viruses. For seasonal influenza viruses, similar transmission has been demonstrated with Syrian hamster, ferret, and guinea pig models [26–28]. Seasonal influenza viruses could be isolated by plaque assay from naive hamsters by day 4 after exposure, whereas SARS-CoV-2 could be detected by RT-PCR in our infected naive hamsters as early as day 4 after exposure [26]. However, in the case of Nipah virus which is more of a neurotropic than respiratory virus, transmission in the Syrian hamster model was largely by direct contact, despite predominant virus shedding in nasal and oropharyngeal secretions [29].

The intensity of exposure may affect the severity of viral infections as has been demonstrated in outbreaks of chickenpox, measles, and poliomyelitis [30–32]. The effect of virus inoculum on the severity of COVID-19 is evident when the histopathological changes and amount of viral N antigen expression in the respiratory tracts of the infected naive hamsters with or without protection by surgical mask partition was compared with those of the virus-challenged hamsters. Besides a virus inoculum of 10^5 plaque-forming units in 100 µL DMEM being instilled intranasally into the challenged hamsters, the inoculum might be aspirated directly into the lungs when the hamsters were under anesthesia. Such large dose of deep exposure resulted in significantly more severe histopathological changes and higher amount of viral N antigen expression in the respiratory tract than the infected naive hamsters after droplet and/or aerosol exposure. The protective effect of masking may not just determine the success or failure of SARS-CoV-2 transmission, but it may also determine the severeity of COVID-19 in the case of successful transmission. For example, in Hong Kong where the population has a mask-use compliance rate of 96.6% during local COVID-19 epidemic, both the incidence rate (1048 cases per 7.5 million population) and crude fatality rate (4 out of 1048, 0.4%) of COVID-19 were among the lowest in the world at the time of writing [33].

Although we could not differentiate whether transmission occurred by respiratory droplets or airborne aerosols in this study, both types of noncontact transmission might have

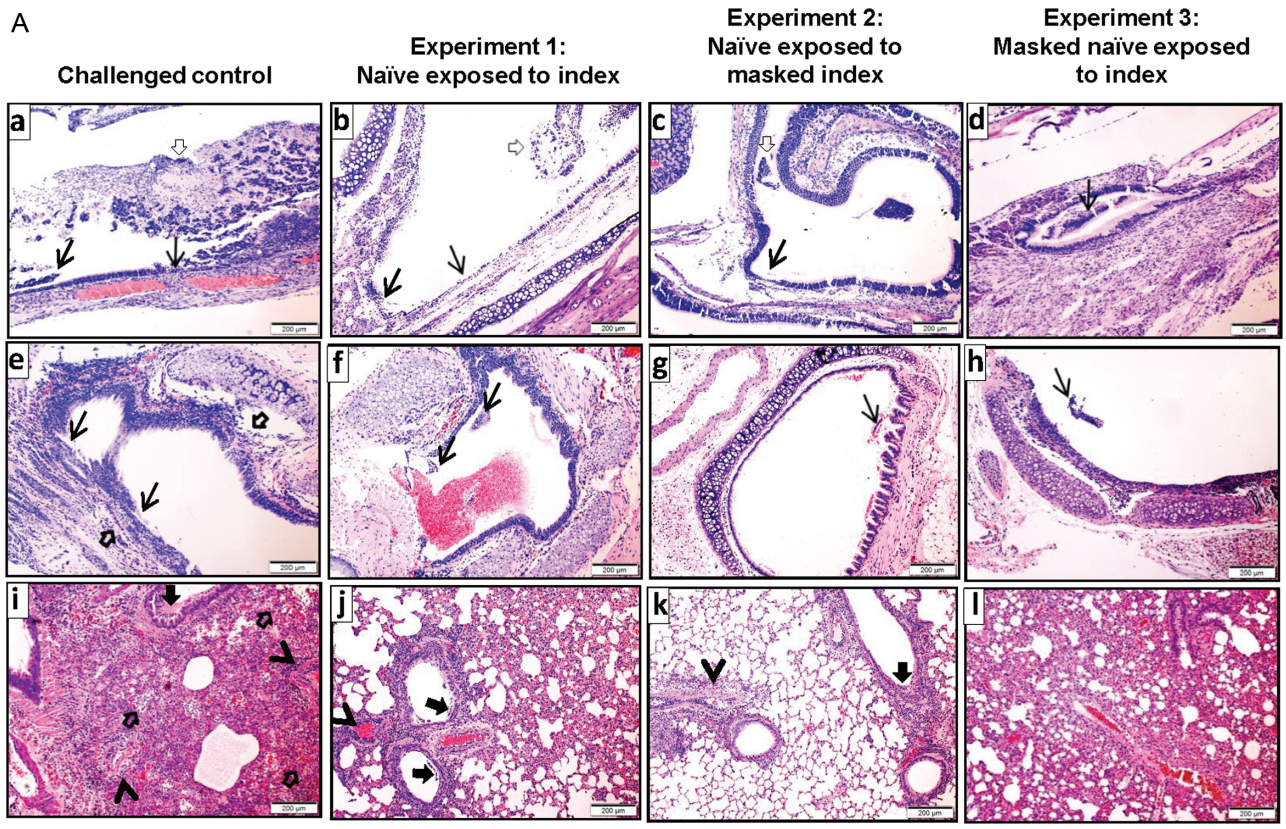

Figure 6. Histopathological changes and SARS-CoV-2 nucleocapsid (N) protein expression in the upper and lower respiratory tissues of the hamsters. *A*, Hematoxylin and eosin-stained tissue sections. (a) to (d) Representative images of nasal turbinate tissue sections which showed pieces of epithelium desquamation (arrows) in all 4 groups of hamsters. The tissue damage was generally more severe in the challenged control hamster, which exhibited massive secretion mixed with detached epithelial cells in the nasal cavity (empty arrow). (e) to (h) Representative images of the tracheal tissue sections showing various degrees of epithelial desquamation (arrows) and submucosal infiltration, which was also more prominent in the challenged control hamster (empty arrows). (i) to (l) Representative images of the lung sections. (i) The lung of the challenged control hamster at 5 dpi showed bronchiolar epithelial cell death, luminal secretion and cell debris (arrow), severe alveolar infiltration, exudation, and hemorrhage (empty arrows). Two blood vessels showed perivascular and intra-endothelial infiltration (arrowheads). (j) The lung of the infected naive hamster from experiment 1 showed bronchiolar epithelial desquamation (arrows), patchy alveolar wall thickening, and blood vessel congestion (arrowhead). (k) Lung of the infected naive hamster from experiment 2 showed no apparent alveolar damage but with bronchiolar epithelial desquamation (arrow) and mild perivascular infiltration (arrowhead). (l) Lung of the infected naive hamster from experiment 3 showed mild alveolar wall thickening with blood vessel congestion. *B*, Immunofluorescence-stained viral N protein expression in hamster respiratory tissues. (a) to (d) Representative images of the nasal turbinate of the hamsters, showing more abundant viral N antigen expression in the challenged control hamster than the infected naive hamsters in experiments 1, 2, and 3. Viral N antigen-positive cells located in the epithelium (arrows) and viral N antigens associated with detached cells (solid arrows). (e) to (h) Tracheal tissue of the challenged control hamster showed more intense epithelial viral N antigen expression (arrows) than the infected naive hamsters in experiments 1, 2, and 3. (i) to (l) Viral N antigen expression in the lung tissues. Lung sections of the challenged control hamster showed diffuse viral N antigen expression in alveolar cells compared to scanty expression in the bronchiolar epithelium (thin arrows) and alveoli (solid arrows) of the infected naive hamsters in experiments 1, 2, and 3. Abbreviations: dpi, days postinoculation; SARS-CoV-2, severe acute respiratory syndrome coronavirus 2.

happened because surgical masks are most efficient in filtering out large respiratory droplets of >10 μm but not the airborne aerosol particles of <5 μm. Therefore, noncontact transmission still occurred in our hamster model despite a reduction of transmission when the naive hamsters were protected by mask partitioning. Alternatively, the filtration efficiency of the masks might have declined over time during the study period. Interestingly, transmission to the exposed naive hamsters was significantly reduced when surgical mask partition was placed to prevent emission of exhaled virus from the challenged index hamsters. This was not completely unexpected because the masking of infectious patients with multidrug-resistant tuberculosis on a hospital ward in South Africa reduced airborne transmission by 56% from these patients to guinea pigs which were breathing the ward air, compared with the percentage of transmission to guinea pigs during periods when masks were not worn [34]. This report clearly showed that surgical masks could be partially effective in reducing the transmission of a well-known airborne pathogen *Mycobacterium tuberculosis* and corroborated with the results of the masking experiments in our hamster model of noncontact transmission of SARS-CoV-2.

Unlike the use of surgical mask in healthcare setting, masking in the community remains controversial. The World Health Organization found no evidence that wearing a surgical mask by healthy persons can prevent acquisition of SARS-CoV-2 [35]. However, the US Centers for Disease Control and

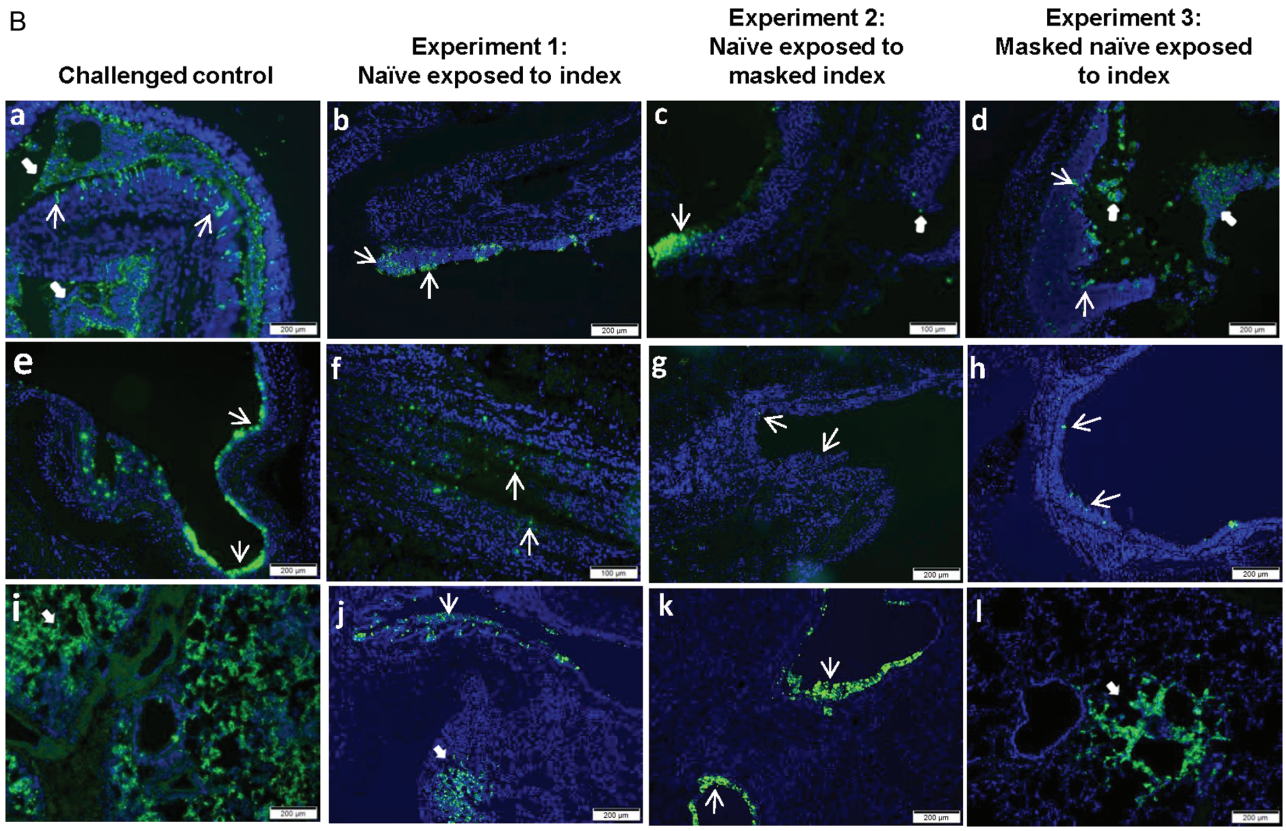

Figure 6. Continued.

Prevention recommends the use of cloth face coverings in communities with significant community-based transmission [36]. This shift of recommendation was based on the finding of pre-symptomatic shedding of SARS-CoV-2 and the presence of asymptomatic patients with high viral loads in the community. Face mask usage may serve as source control by preventing dispersal of droplets during talking, sneezing, and coughing, and also reduce the risk of environmental contamination by SARS-CoV-2. Our results showed that masking of the challenged index appeared to be more important than masking the to-be-exposed healthy hamsters, which is consistent with the findings in a systematic review on influenza transmission [37]. Masking is a continuous form of protection to stop the spreading of saliva and respiratory droplets to or from others, and to or from the environment to the susceptible individuals by hands through subconscious touching of their nose, mouth, and eyes. Hand hygiene is always the cornerstone to prevent transmission of SARS-CoV-2, but it is a one-off discontinuous process where hand contamination may occur again easily between each episode of alcoholic hand rubbing or hand washing. It has also been shown that wearing a mask with frequent hand hygiene significantly reduced transmission of seasonal influenza virus in the community setting [38]. But once the effect of the use of surgical mask was removed, the effect of hand hygiene became insignificant [38].

Containment public health interventions including border source control, extensive testing of cases and isolation, rapid contact tracing and quarantine, and mitigation measures of social distancing including school closures, home office, closure of food premises and public places to stop gatherings and even city lockdown, were used by every developed country at different time points and to different extents to control the COVID-19 pandemic. However, the presence of a significant proportion of asymptomatically infected patients who were not aware of the need of testing, wearing mask, or isolation has markedly impaired these control measures. In the case of the Princess Diamond cruise outbreak, 6 out of 9 returnees were found to be asymptomatically infected during the 14 days of quarantine and serial virological monitoring after returning to Hong Kong [39]. Our findings on the use of surgical mask partition for protection against noncontact transmission in this hamster model supported the use of community-wide masking to reduce the amount of virus shedding from the asymptomatically infected patients and to protect susceptible individuals. This should be a reasonable approach for the epidemic control of a densely populated city like Hong Kong without resorting to city lockdown, and an important measure during the stepwise loosening of social distancing measures in the days ahead.

Our study had limitations. The speed of the unidirectional airflow could not be unified when the surgical mask partitions

were installed, but that would also apply when surgical masks were worn by different individuals in real life, and this could indeed be a mechanism for protection during mask usage. We could not determine the exact timing of acquisition of SARS-CoV-2 by the exposed naive hamsters as we only started sampling them 4 days after exposure. Moreover, we could not determine if contact transmission has occurred among exposed naive hamsters housed in the same cage. This might have resulted in an underestimation of the protective efficacy of masks, which would otherwise be even more significant. Further studies on the relative importance of large respiratory droplets and small airborne aerosols are warranted.

Notes

Acknowledgement. We sincerely thank the staff of the Laboratory Animal Unit of The University of Hong Kong and the Laboratory Animal Service Centre of The Chinese University of Hong Kong for their facilitation of the study.

Author contributions. J. F.-W. C., S. Y., A. J. Z., and K.-Y. Y. had roles in the study design, data collection, data analysis, data interpretation, and writing of the manuscript. V. K.-M. P. and C. C.-S. C. had roles in the study design, experiments, data collection, data analysis, and data interpretation. A. C.-Y. L., Z. F., C. L., R. L., J. C., K. T., C. L., V. C.-C. C., J.-P. C., H. C., K.-H. C., K. K.-W. T., and S. S. had roles in the experiments, data collection, data analysis, and/or data interpretation. All authors reviewed and approved the final version of the manuscript.

Disclaimer. The funding sources had no role in the study design, data collection, analysis, interpretation, or writing of the report.

Financial support. This study was partly supported by the donations of May Tam Mak Mei Yin, Richard Yu and Carol Yu, the Shaw Foundation Hong Kong, Michael Seak-Kan Tong, Respiratory Viral Research Foundation Limited, Hui Ming, Hui Hoy and Chow Sin Lan Charity Fund Limited, Chan Yin Chuen Memorial Charitable Foundation, Marina Man-Wai Lee, the Hong Kong Hainan Commercial Association South China Microbiology Research Fund, the Jessie & George Ho Charitable Foundation, Perfect Shape Medical Limited, and Kai Chong Tong; and funding from the Health and Medical Research Fund (grants COVID190121 and COVID190123), the Food and Health Bureau, The Government of the Hong Kong Special Administrative Region; the National Program on Key Research Project of China (grants 2020YFA0707500 and 2020YFA0707504); the Consultancy Service for Enhancing Laboratory Surveillance of Emerging Infectious Diseases and Research Capability on Antimicrobial Resistance for Department of Health of the Hong Kong Special Administrative Region Government; the Theme-Based Research Scheme (T11/707/15) of the Research Grants Council, Hong Kong Special Administrative Region; Sanming Project of Medicine in Shenzhen, China (SZSM201911014); and the High Level-Hospital Program, Health Commission of Guangdong Province, China.

Potential conflicts of interests. The authors: No reported conflicts of interest. All authors have submitted the ICMJE Form for Disclosure of Potential Conflicts of Interest.

References

1. Peiris JS, Lai ST, Poon LL, et al; SARS study group. Coronavirus as a possible cause of severe acute respiratory syndrome. Lancet **2003**; 361:1319–25.
2. Lau SK, Woo PC, Li KS, et al. Severe acute respiratory syndrome coronavirus-like virus in Chinese horseshoe bats. Proc Natl Acad Sci U S A **2005**; 102:14040–5.
3. Ge XY, Li JL, Yang XL, et al. Isolation and characterization of a bat SARS-like coronavirus that uses the ACE2 receptor. Nature **2013**; 503:535–8.
4. Chan JF, To KK, Tse H, Jin DY, Yuen KY. Interspecies transmission and emergence of novel viruses: lessons from bats and birds. Trends Microbiol **2013**; 21:544–55.
5. Chan JF, Lau SK, To KK, Cheng VC, Woo PC, Yuen KY. Middle East respiratory syndrome coronavirus: another zoonotic betacoronavirus causing SARS-like disease. Clin Microbiol Rev **2015**; 28:465–522.
6. Zhu N, Zhang D, Wang W, et al; China Novel Coronavirus Investigating and Research Team. A novel coronavirus from patients with pneumonia in China, 2019. N Engl J Med **2020**; 382:727–33.
7. Zhou P, Yang XL, Wang XG, et al. A pneumonia outbreak associated with a new coronavirus of probable bat origin. Nature **2020**; 579:270–3.
8. Chan JF, Kok KH, Zhu Z, et al. Genomic characterization of the 2019 novel human-pathogenic coronavirus isolated from a patient with atypical pneumonia after visiting Wuhan. Emerg Microbes Infect **2020**; 9:221–36.
9. Chan JF, Yuan S, Kok KH, et al. A familial cluster of pneumonia associated with the 2019 novel coronavirus indicating person-to-person transmission: a study of a family cluster. Lancet **2020**; 395:514–23.
10. Huang C, Wang Y, Li X, et al. Clinical features of patients infected with 2019 novel coronavirus in Wuhan, China. Lancet **2020**; 395:497–506.
11. To KK, Tsang OT, Leung WS, et al. Temporal profiles of viral load in posterior oropharyngeal saliva samples and serum antibody responses during infection by SARS-CoV-2: an observational cohort study. Lancet Infect Dis **2020**; 20:565–74.
12. Wichmann D, Sperhake JP, Lutgehetmann M, et al. Autopsy findings and venous thromboembolism in patients with COVID-19: a prospective cohort study. Ann Intern Med **2020**. doi: 10.7326/M20-2003. [Epub ahead of print]
13. Connors JM, Levy JH. COVID-19 and its implications for thrombosis and anticoagulation. Blood **2020**. doi: 10.1182/blood.2020006000. [Epub ahead of print]
14. Cheung KS, Hung IF, Chan PP, et al. Gastrointestinal manifestations of SARS-CoV-2 infection and virus load in fecal samples from the Hong Kong cohort and systematic review and meta-analysis. Gastroenterology **2020**. doi: 10.1053/j.gastro.2020.03.065. [Epub ahead of print]
15. Jones VG, Mills M, Suarez D, et al. COVID-19 and Kawasaki disease: novel virus and novel case. Hosp Pediatr **2020**. doi: 10.1542/hpeds.2020-0123. [Epub ahead of print]
16. Toscano G, Palmerini F, Ravaglia S, et al. Guillain-Barre syndrome associated with SARS-CoV-2. N Engl J Med **2020**. doi: 10.1056/NEJMc2009191. [Epub ahead of print]
17. Guan WJ, Ni ZY, Hu Y, et al; China Medical Treatment Expert Group for Covid-19. Clinical characteristics of coronavirus disease 2019 in China. N Engl J Med **2020**; 382:1708–20.
18. Vaira LA, Salzano G, Deiana G, De Riu G. Anosmia and Ageusia: common findings in COVID-19 patients. Laryngoscope **2020**. doi: 10.1002/lary.28692. [Epub ahead of print]
19. World Health Organization. Coronavirus disease (COVID-2019) situation reports: situation report - 112. Available at: https://www.who.int/docs/default-source/coronaviruse/situation-reports/20200511-covid-19-sitrep-112.pdf?sfvrsn=813f2669_2. Accessed 12 May 2020.
20. Chan JF, Zhang AJ, Yuan S, et al. Simulation of the clinical and pathological manifestations of coronavirus disease 2019 (COVID-19) in golden Syrian hamster model: implications for disease pathogenesis and transmissibility. Clin Infect Dis **2020**. doi: 10.1093/cid/ciaa325. [Epub ahead of print]
21. Chu H, Chan JF, Yuen TT, et al. An observational study on the comparative tropism, replication kinetics, and cell damage profiling of SARS-CoV-2 and SARS-CoV: implications for clinical manifestations, transmissibility, and laboratory studies of COVID-19. Lancet Microbe **2020**. doi: 10.1016/S2666-5247(20)30004–5.
22. Chan JF, Chan KH, Choi GK, et al. Differential cell line susceptibility to the emerging novel human betacoronavirus 2c EMC/2012: implications for disease pathogenesis and clinical manifestation. J Infect Dis **2013**; 207:1743–52.
23. Zhou J, Chu H, Li C, et al. Active replication of Middle East respiratory syndrome coronavirus and aberrant induction of inflammatory cytokines and chemokines in human macrophages: implications for pathogenesis. J Infect Dis **2014**; 209:1331–42.
24. Chu H, Chan JF, Wang Y, et al. Comparative replication and immune activation profiles of SARS-CoV-2 and SARS-CoV in human lungs: an ex vivo study with implications for the pathogenesis of COVID-19. Clin Infect Dis **2020**; 71:1400–409.
25. Chan JF, Yip CC, To KK, et al. Improved molecular diagnosis of COVID-19 by the novel, highly sensitive and specific COVID-19-RdRp/Hel real-time reverse transcription-PCR assay validated in vitro and with clinical specimens. J Clin Microbiol **2020**; 58:e00310–20.
26. Iwatsuki-Horimoto K, Nakajima N, Ichiko Y, et al. Syrian Hamster as an animal model for the study of human influenza virus infection. J Virol **2018**; 92:e01693–17.
27. Jayaraman A, Pappas C, Raman R, et al. A single base-pair change in 2009 H1N1 hemagglutinin increases human receptor affinity and leads to efficient airborne viral transmission in ferrets. PLoS One **2011**; 6:e17616.
28. Seibert CW, Rahmat S, Krause JC, et al. Recombinant IgA is sufficient to prevent influenza virus transmission in guinea pigs. J Virol **2013**; 87:7793–804.
29. de Wit E, Bushmaker T, Scott D, Feldmann H, Munster VJ. Nipah virus transmission in a hamster model. PLoS Negl Trop Dis **2011**; 5:e1432.

30. Garenne M, Aaby P. Pattern of exposure and measles mortality in Senegal. J Infect Dis **1990**; 161:1088–94.
31. Poulsen A, Cabral F, Nielsen J, et al. Varicella zoster in Guinea-Bissau: intensity of exposure and severity of infection. Pediatr Infect Dis J **2005**; 24:102–7.
32. Nielsen NM, Aaby P, Wohlfahrt J, Pedersen JB, Melbye M, Mølbak K. Intensive exposure as a risk factor for severe polio: a study of multiple family cases. Scand J Infect Dis **2001**; 33:301–5.
33. Cheng VC, Wong SC, Chuang VW, et al. The role of community-wide wearing of face mask for control of coronavirus disease 2019 (COVID-19) epidemic due to SARS-CoV-2. J Infect **2020**. doi: 10.1016/j.jinf.2020.04.024. [Epub ahead of print]
34. Dharmadhikari AS, Mphahlele M, Stoltz A, et al. Surgical face masks worn by patients with multidrug-resistant tuberculosis: impact on infectivity of air on a hospital ward. Am J Respir Crit Care Med **2012**; 185:1104–9.
35. World Health Organization. Advice on the use of masks in the context of COVID-19: interim guidance, **2020**. Available at: https://apps.who.int/iris/handle/10665/331693. Accessed 11 May 2020.
36. Centers for Disease Control and Prevention. Recommendation regarding the use of cloth face coverings, especially in areas of significant community-based transmission. Available at: https://www.cdc.gov/coronavirus/2019-ncov/prevent-getting-sick/cloth-face-cover.html. Accessed 11 May 2020.
37. Cowling BJ, Zhou Y, Ip DK, Leung GM, Aiello AE. Face masks to prevent transmission of influenza virus: a systematic review. Epidemiol Infect **2010**; 138:449–56.
38. Wong VW, Cowling BJ, Aiello AE. Hand hygiene and risk of influenza virus infections in the community: a systematic review and meta-analysis. Epidemiol Infect **2014**; 142:922–32.
39. Hung IF, Cheng VC, Li X, et al. COVID-19 in its making during quarantine after release from a cruise ship: a cohort study on SARS-CoV-2 shedding and seroconversion. Lancet Infect Dis **2020**. [accepted and in press]